

THE IMPACT OF THE CASCADING STRUCTURE OF PRECIPITATION ON REFLECTIVITY MEASUREMENTS

Dominik Jacques*, P. Borque, J. Yip, W. Chang and F. Fabry
J. S. Marshall Radar Observatory, McGill University, Canada

1. INTRODUCTION

We are investigating the possible effects of structured precipitation fields on the intensity estimates of weather radar echoes.

To motivate this research we will first introduce the equation describing the fluctuating intensity $I(t)$ of radar echoes given a constantly reorganizing field of targets (Lhermitte 1960).

$$I(t) = \sum_i a_i^2 + \sum_i \sum_j a_i a_j \cos(\phi_i - \phi_j) \quad (1)$$

In this equations, a_i and a_j represent the amplitude of the wave backscattered by individual targets. For simplicity, the Doppler phase shift caused by the movements of targets has been neglected.

The first term of (1) is due to incoherent scattering and will be proportional to the number of scatterers in the resolution volume. This quantity allows the meaningful estimation of reflectivity from radar echoes.

The second term describes the intensity fluctuations due to coherent scattering. As hydrometeors reorganise themselves, the constructive and destructive interference of their returns will influence the measured intensity. If the phase ϕ_i of each hydrometeor is independently and uniformly distributed between 0 and 2π , then the expected value of this term will be zero. This explains how time integration of radar intensity measurements greatly reduce the influence of this second term, allowing the estimation of reflectivity (Marshall and Hitschfeld 1953).

We can demonstrate this by performing a simple experiment. This example will illustrate why time integration of radar echoes is important and introduce some of the methodology used later.

2. TIME INTEGRATION OF RADAR ECHOES

We can picture the front of a radar wave as a surface traversing a resolution volume at the speed

*Corresponding author address: Dominik Jacques, Univ. McGill, Dept. Atmospheric and Oceanic Sciences, Montreal, Qc, H3A 2K6; e-mail: dominik.jacques@mail.mcgill.ca.

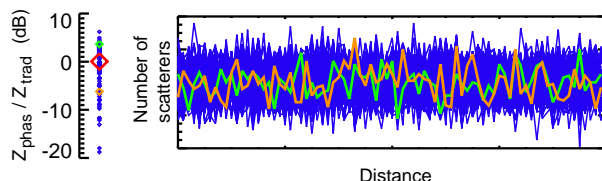


Figure 1: Estimates of intensity for 100 randomly generated fields of uniformly distributed scatterers. For each field the ratio Z_{phas}/Z_{true} was computed and is displayed in the left plot. Examples of two fields and their respective ratio are displayed in green and yellow. The mean ratio value (0.04 dB) is displayed in red.

of light. The echoes of all the scatterers illuminated at a given instant (and a given distance) by that front will have the same phase. In this case, a 1D vector representing the number of drops found at a given distance d from the radar, will be sufficient to describe the spatial distribution of hydrometeors.

One hundred such vectors are illustrated in Fig. 1. For clarity, two of these vector have been highlighted in colors. In each case, a constant number of drops was randomly distributed along the vector with equiprobable chances of finding itself at any distance d along the vector.

In reality the drops are continuously distributed in space. For this experiment however, we let the scatterers be separated by a fixed distance of $\lambda/8$. This allowed phase interactions to occur while keeping the computational aspects simple.

From these vectors of scatterers, it was then possible to compute the returned intensity in two different ways.

In the first case, the phase of raindrop echoes ϕ_i (in radians) given by

$$\phi_i = 2\pi \left(\frac{2d_i}{\lambda} \right) \quad (2)$$

was taken into account. The reflectivity Z was

computed using

$$Z_{phase} = \frac{2}{c\tau} \left[\left(\sum_{n=1}^N a_i \cos \phi_i \right)^2 + \left(\sum_{n=1}^N a_i \sin \phi_i \right)^2 \right]. \quad (3)$$

In this equation, c is the speed of light, τ is the radar pulse length and N is the total number of drops in the considered resolution volume. For simplicity, we let $a_i = 1$. This quantity corresponds to what would actually be measured by a weather radar illuminating this field.

In the second case, we let the intensity be proportional to the number of hydrometeors. This is the unknown ‘true’ reflectivity being sought from weather radar measurements without the influence of coherent scattering. The calculated ‘true’ reflectivity is given by

$$Z_{true} = \frac{2}{c\tau} \sum_{i=1}^N a_i = \frac{2}{c\tau} N. \quad (4)$$

The ratio $10 \log_{10}(Z_{phase}/Z_{true})$ will be indicative of the error induced by assuming that the second term of (1) is zero when Z_{phas} is measured.

When computed from individual fields (in color, Fig. 1) this ratio is likely to differ from zero. However, when 100 such fields are considered $\langle Z_{phase} \rangle$ the average of the reflectivity taking the phase into account becomes very similar to Z_{true} . Then $10 \log_{10}(\langle Z_{phase} \rangle / \langle Z_{true} \rangle) \approx 0$ dB as illustrated by the red diamond in Fig. 1. This result verifies that for randomly generated fields with a uniform distribution, the second term of (1) vanishes when many measurements of a reorganizing field are averaged.

3. STRUCTURED FIELDS

Turbulence studies have shown that wind fields possess a cascading structure at all scales down to the order of millimeters (Kolmogorov 1941). It has also been demonstrated that falling precipitation conforms to this structure down to scales where drop sorting and inertia have a stronger effect than advection by the wind. This is illustrated in Fig. 2 where the power spectra of precipitation are depicted for rain, ice pellets and snow (Fabry 1996). In each case, we see the cascading structure of precipitation in the form of a sloping power spectra. At scales between a hundred to a few tens of meters the slope abruptly becomes horizontal indicating a loss of structure. We will refer to this break in

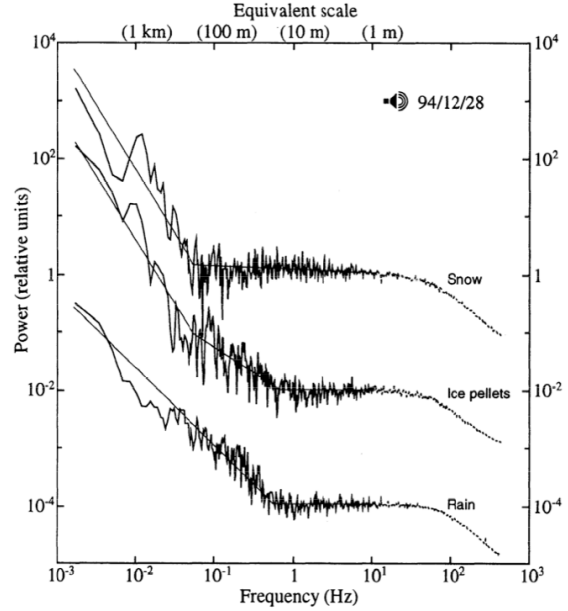


Figure 2: Normalized power spectra of precipitation in snow, ice pellets and rain. The dashed lines above 10Hz indicate spatial scales smaller than the sensor size. These spectra have been shifted for display. Adapted from Fabry (1996).

the scaling properties of precipitation fields as the breakup scale.

In (2) we can see that constructive wave interferences will be created at the scale of half the radar wavelength (λ). As demonstrated by Fabry (1996), the breakup scales of precipitation fields are much larger than the ≈ 10 cm wavelength of a typical scanning radar. It could then be argued that the scaling properties of precipitation should not affect reflectivity measurements.

However, the presence of structure in precipitation fields violates the assumption that scatterers are independently and uniformly distributed in space. Because of the double summation in the second term of (1), even small contamination by structure could lead to significant offsets in intensity estimations.

We can speculate that the closer the breakup scale will be to the radar wavelength, the more structure should affect estimations of intensity. This situation will occur for radars having long wavelengths (as is the case for wind profilers) or when the breakup scale is small (in the case of clouds droplets for example).

To answer these interrogations we will compute $10 \log_{10}(\langle Z_{phase} \rangle / \langle Z_{true} \rangle)$ from fields

possessing structure and breakup scales similar to real precipitation fields.

4. METHODOLOGY

We first needed to construct fields exhibiting characteristics similar to those of Fig. 2.

As a start point, we used a 2D field (Fig. 3, top) possessing the $1/f^{1.4}$ cascading structure observed in precipitation over all scales (Fig. 2). This matrix was then reduced to 1D vector by computing the total number of ‘drops’ in every column (Fig. 3, bottom).

Different parameters had to be adjusted to make this simulation realistic. The spacing between the vector points was set to 1.25 cm corresponding to $\lambda/8$ for a 10 cm wavelength radar. In accordance with these dimension, the total number of drops was set to match a typical values of 1000 drops per meter cube (Rogers and Yau 1989).

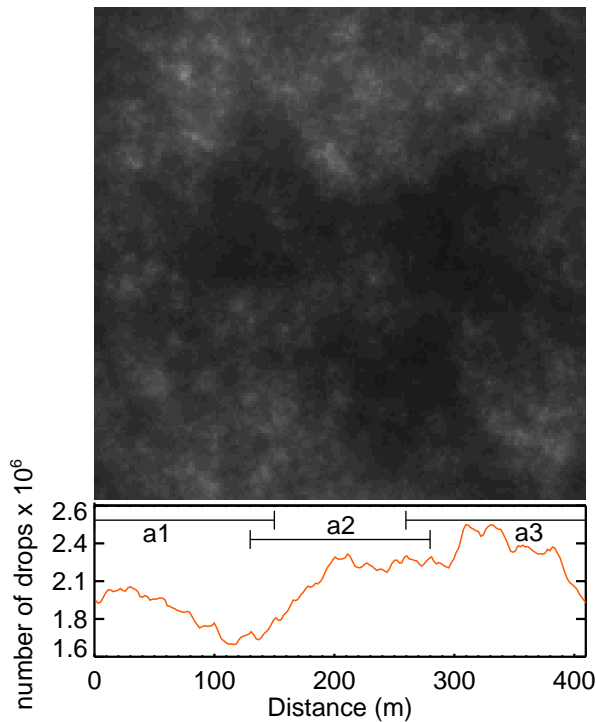


Figure 3: Original 2D field exhibiting structure at all scales (top) and its reduction to a 1D vector (bottom) by the summation of all columns. a1, a2 and a3 are subsections of this field for which reflectivity was analysed.

The cascading structure of this initial field can be observed from its power spectrum (Fig. 4 in orange).

Unlike precipitation, this field possesses structure up to the smallest scales.

To recreate the breakup scale observed in precipitation, individual raindrops were randomly ‘shuffled’ around their initial position. The distance by which drops would be displaced was set following a normal distribution with mean zero and a standard deviation σ .

The effect of this shuffling process is depicted in Fig. 4, where the power spectra of the shuffled fields (in blue) are compared to the spectrum of the initial field (in orange). These graphs show that the structure of the simulated precipitation fields is lost at roughly twice the σ chosen.

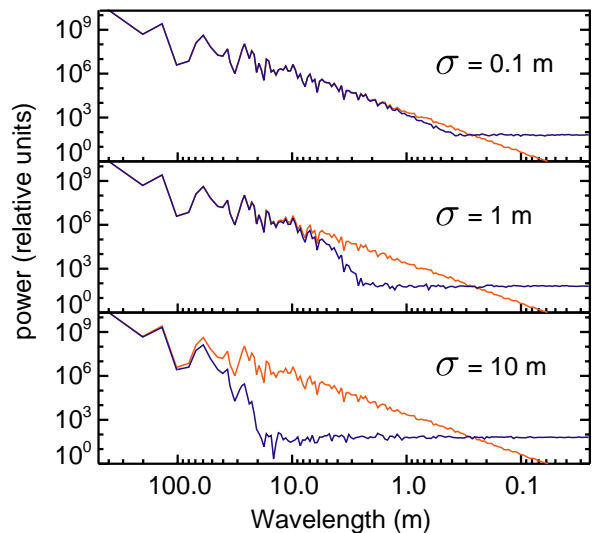


Figure 4: Power spectra of hydrometeor fields that have been shuffled (blue) using different σ in comparison with the power spectrum of the original field (orange).

The random aspect of the shuffling process is important so that 100 different fields could be computed from one initial vector at every chosen σ . Averaging the simulated returns from all these field is then equivalent to averaging the fluctuating echoes of a weather radar.

5. RESULTS AND DISCUSSION

Figure 5 illustrates the effect of structure on reflectivity estimations for different subsections (a1, a2, a3) of the shuffled fields. Each of these sections represents a distance of 150 m, the range resolution of a radar having a pulse width of $1 \mu\text{s}$. The reflectivity ratio of each of the one hundred

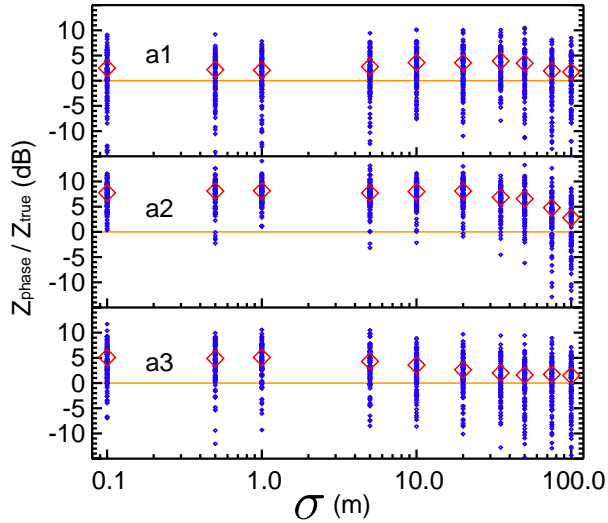


Figure 5: Z_{phase}/Z_{true} for one hundred shuffled fields (blue diamonds) and their mean (red diamonds) for different σ computed from three different subsections (a1, a2, a3) of the original field.

randomly generated field (blue diamonds) and their mean (red diamonds) for different σ were plotted. Significant variations with respect to both the scale of the structure breakup (the different σ) and the different area considered could be observed.

For $\sigma < 50$ m a positive bias of reflectivity estimations could be observed. This bias appears to depend on the presence of gradients in the spatial distribution of drops.

For $\sigma > 50$ m a positive bias can also be observed but it is much smaller. This graph confirms that the breakup scale do impact on reflectivity estimations. However, because of the variability observed between the different fields considered, it is hard to assess the exact nature of this effect.

We suspected that the perfectly square radar pulse used in our simulations might be causing the variations between subsections. Such pulse should make the radar very sensitive to reflectivity measurement over uneven number of wavelengths. To test this hypothesis, we performed our computation for imbalanced pairs of phase measurements.

Figure 6 shows the reflectivity ratio computed in the subsection a2. Only this time, we added a few data points so that the reflectivity was computed from an uneven number of wavelengths. Whenever the pairs were unbalanced, the reflectivity ratio was higher than 20 dB. Adding enough points to balance the phases (in the $\lambda/2$ case) yielded the same ratios found in Fig. 5. It appeared that mea-

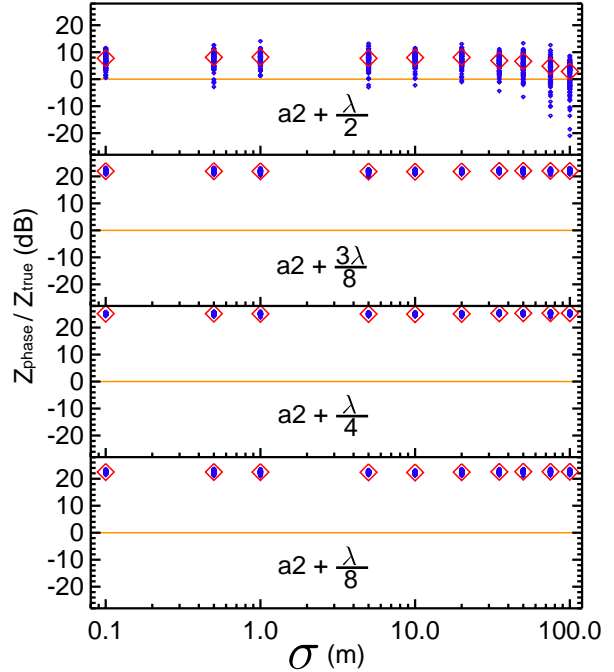


Figure 6: Reflectivity ratio computed using uneven number of wavelengths. For this graph, only the area a2 was considered but this time, data points were added one at a time.

surements performed from uneven fractions of λ are very much overestimated when the phase is taken into account. Perhaps this effect could be exploited to increase radar sensitivity in some way.

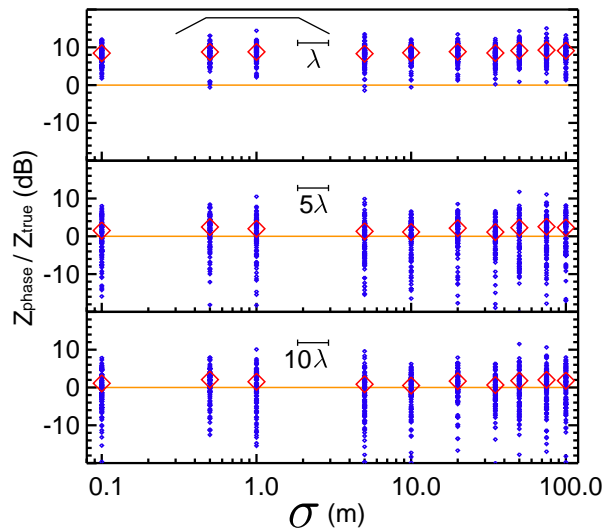
In reality, radar pulses are not perfectly square. To make our simulation more realistic we recomputed same reflectivity ratios but this time we gave the radar pulse a trapezoidal shape (Fig. 7). The field chosen for this experiment is the one where we added $\lambda/4$ which displayed the most drastic over-estimation of reflectivity.

With a rise/fall time of 1λ the reflectivity biases were now less than 10 dB. This also removed all dependence on the breakup scale. With a rise/fall time of 10λ the reflectivity ratio practically falls to zero for all σ .

6. CONCLUSION

For precipitation fields having breakup scale larger than 100 m, taking the phase into account does not appear affect the reflectivity measurements for a S-band radar having a pulse width of $1 \mu s$.

Given a perfectly square pulse, a radar would be very sensitive to measurements taken over uneven



Rogers, R. R. and M. K. Yau, 1989: *A Short Course in Cloud Physics*. Butterworth Heinmann, third edition edition.

Figure 7: Using the field computed over unbalanced phase pairs (Fig. 6, center) the reflectivity ratio computed with a simulated trapezoidal pulse shape with a rise/fall time of 1, 5 and 10 λ .

number of wavelengths. This effect disappears in the presence of a trapezoidal radar pulse having a rise and fall time of a few wavelengths. The trapezoidal shape also makes the reflectivity ratio independent from the breakup scale of precipitation.

Acknowledgement

Thanks to Valliappa Lakshmanan of NSSL for making his AMS Latex style file available on the web.

References

- Fabry, F., 1996: On the determination of scales ranges for precipitation fields. *Journal of Geophysical research*, **101**, 12 819–12 826.
- Kolmogorov, A., 1941: The local structure of turbulence in incompressible viscous fluid for very large reynolds numbers. *C. R. Acad. Sci. U.S.S.R.*, **30**, 301–306.
- Lhermitte, R. M., 1960: New developments of the echo fluctuation theory and measurements. *preprints of the 8th weather radar conference*, pp. 263-268.
- Marshall, J. S. and W. Hitschfeld, 1953: interpretation of the fluctuating echo from randomly distributed scatterers. part 1. *Canadian Journal of Physics*, **31**, 962–994.